Korean J. Chem. Eng., 36(8), 1249-1257 (2019)
DOI: 10.1007/s11814-019-0307-x

pISSN: 0256-1115
eISSN: 1975-7220

Effects of regeneration conditions on sulfated CuSSZ-13 catalyst for NH_3-SCR

Meiqing Shen*,,***, Zhixin Wang*, Xinhua Li*, Jiaming Wang*, Jianqiang Wang*, Chen Wang****,†, and Jun Wang*,†**

*Key Laboratory for Green Chemical Technology of State Education Ministry, School of Chemical Engineering & Technology, Tianjin University, Tianjin 300350, P. R. China
**Collaborative Innovation Centre of Chemical Science and Engineering (Tianjin), Tianjin 300350, P. R. China
***State Key Laboratory of Engines, Tianjin University, Tianjin 300350, P. R. China
****School of Environmental and Safety Engineering, North University of China, Taiyuan 030051, P. R. China
(*Received 13 February 2019 • accepted 21 May 2019*)

Abstract−To understand the role of regeneration conditions on sulfur-poisoned Cu/SSZ-13 catalysts for NH_3-SCR, the physicochemical characterizations and NO_x conversions were investigated. The sulfur-poisoned Cu/SSZ-13 catalysts were treated at different conditions as a function of temperature and duration. TGA results revealed that regeneration at 500 °C only removed parts of sulfur spices and at 700 °C can completely remove all sulfur spices. The physical structural characterizations results illustrate that regeneration below 700 °C has no significant impact on CHA structure for Cu/SSZ-13 catalysts, while dealumination occurs on poisoned Cu/SSZ-13 when regeneration temperature is higher than 700 °C. EPR and H_2-TPR results show that the sulfate decomposition and Cu migration reactions involved during regeneration and, as a result, the content of Cu^{2+} gradually increased as the extent of regeneration increased. The kinetics tests support that NO_x conversion recovery is related to the content of Cu^{2+} increase during regeneration. Our study reveals that the optimum regeneration temperature is 700 °C, because severe dealumination at 750 °C inhibited Cu^{2+} amount increase.

Keywords: Cu/SSZ-13, NH_3-SCR, Sulfur Poisoning, Regeneration, Cu Species

INTRODUCTION

A lean burn diesel engine can improve fuel efficiency; however, nitrogen oxides (NO_x) generated by the engine will lead to air pollution. To meet more and more stringent emission regulations, ammonia selective catalytic reduction (NH_3-SCR) has been found to be an effective solution to reduce the NO_x emission [1]. V_2O_5/WO_3-TiO_2, Cu-based zeolites, such as Cu/ZSM-5 and Cu/beta, are representative catalysts for NH_3-SCR technology [2-4]. Chabazite(CHA)-structured small-pore zeolite catalysts, especially for Cu/SSZ-13 catalysts, have received wide public attention for their wide temperature window and excellent hydrothermal stability [5-10].

There exist some sulfur-containing species in fuel that will hinder the catalysts application, which would form sulfur oxides through combustion. Sulfur oxides could lead to severe deactivation for Cu/CHA NH_3-SCR catalysts, and the poisoned catalysts cannot remove NO_x effectively to meet emission regulations [11-13]. So far, the deactivation mechanism of sulfur oxides has been of great concern to many researchers [11-13]. Su et al. investigated the sulfur species in sulfur-poisoned Cu/CHA catalyst and found that there are mainly H_2SO_4, $Al_2(SO_4)_3$ and $CuSO_4$, which affect the low temperature activity of catalyst [12]. Jangjou et al. added SO_2 to the feed gas to conduct the study on how Cu/SSZ-13 catalyst is poisoned by SO_2. The studies show that $CuOH^+$ is more feasible to react with SO_2 and forms stable Cu-S species during sulfation process. Cu-NH_3-S and Cu-S species are formed during the sulfation process, which diminishes catalyst activity. Among all Cu-S species, $CuSO_4$ is more stable, which seriously affects the catalyst activity [14]. Hammershøi et al. investigated the properties of deactivation by sulfation, which is divided in two parts: reversible deactivation and irreversible deactivation. Irreversible deactivation is related to stable Cu-S species [13]. They explored the mechanism of the sulfation process by changing sulfation temperature and duration. They thought that SO_2 is first adsorbed on the catalyst and then oxidized to SO_3. Moreover, they pointed out that SO_2 fluxes mainly affect reversible deactivation; however, irreversible deactivation exists with catalyst with very low sulfur flux, which is related to the Cu-S species with high stability [15]. Wang et al. investigated the effect of different temperature and gas composition on Cu/SAPO-34 during sulfation process. They found that the Cu-SO_4 and Cu-ammonia sulfate species forms in sulfur poisoned catalyst, which leads to a decrease of activity for the catalyst [16]. To sum up, the inferior SCR performance of sulfated catalysts is related to sulfur-species formation (Cu-SO_4 and Cu-ammonia sulfate like).

Naturally, if the Cu/CHA has been poisoned by these sulfur species, the conventional method is to regenerate the poisoned catalysts under hydrothermal condition, as water always co-exists in the exhaust. For Cu/CHA NH_3-SCR catalysts, the widely accepted fact is that Cu-ammonia sulfate-like species could easily be removed at low temperature (lower than 500 °C) and Cu-SO_4 species need much higher temperature to decompose (high than 550 °C). In fact, the efficiency of regeneration is directly correlated to the stable Cu-SO_4

†To whom correspondence should be addressed.
E-mail: wangjun@tju.edu.cn, chenwang87@nuc.edu.cn
Copyright by The Korean Institute of Chemical Engineers.

species and, therefore, desulfation process of Cu-SO_4 species should be paid more attention. To the best of our knowledge, there are few studies focusing on the desulfation process of Cu-SO_4 species on Cu/CHA catalysts. Shen et al. found all amounts of copper sulfate require a high hydrothermal temperature at 750 °C for 12 h to fully decompose and all the poisoned copper could return to the exchange sites on Cu/SAPO-34. And as a result, the poisoned Cu/SAPO-34 could fully recover its SCR performance [17]. However, for Cu/SSZ-13 catalysts, dealumination will occur on Cu/SSZ-13 when hydrothermal aging at 750 °C and will further impact on SCR performance because dealumination process should influence the acid sites (Cu^{2+} and -OH) [18]. Facing this trade-off relationship between full sulfate removal and dealumination over Cu/SSZ-13 catalysts under common condition at hydrothermal aging for diesel, it is necessary to probe the optimum regeneration condition. Besides that, the other unclear information is the desulfation mechanism about stable metal sulfate. What is the decomposition process of Cu-SO_4 species? Why does SCR activity recover after sulfate species decomposition and how does dealumination effect the recovery?

To better answer all the queries we raise in this work, we investigated the effect of regeneration conditions as a function of temperature and time on sulfated Cu/SSZ-13 catalysts poisoned in SO_2 containing feed. SEM and TEM were used to investigate the change of catalysts texture. XRD, DRIFTs, ^{29}Si and ^{27}Al NMR were used to investigate the change of catalyst structure in the regeneration process. We also conducted TGA, H_2-TPR and EPR experiments to investigate the change of Cu species, including isolate Cu^{2+} in two different sites (six-membered ring and CHA cage), CuO and copper sulfate. Finally, we carried out NH_3-SCR experiments and kinetics experiments to obtain the structure-activity relationship of regenerated Cu/SSZ-13 catalysts. The results of this research are critical for improving SCR activity of sulfated Cu/SSZ-13 catalyst, and would provide guidance to design the protocol for protecting SCR deterioration.

EXPERIMENTAL

1. Catalyst Preparation

The Cu/SSZ-13 catalysts were synthesized via a three-step method. The Na/SSZ-13 was synthesized via a hydrothermal method with a mole composition of 1 SiO_2 : 0.067 Al_2O_3 : 0.1 NaOH : 0.1 SDA : 20 H_2O. The silicon source is ludox (25 wt% SiO_2, Qingdao Jiyida Silica Reagent Factory, China), aluminium source is pseudo boehmite (62 wt% Al_2O_3, Shangdong Aluminium Industry Co., Ltd., China), and the structure-directing agent is TMAda-OH (25 wt%, Sinopec Qilu Petrochemical Co., Ltd., China). First, SDA and NaOH liquid were mixed, then pseudo boehmite was added, the gel was stirred for 1 h. Then the gel was added with ludox and stirred for 0.5 h. Thereafter, water was added and stirred for another 0.5 h to get the resulting gel. The resulting gel was put in a stainless steel reactor with Teflon lining and placed in 160 °C for 96 h to crystallize. After the crystallization process, the solid was separated from mother liquor and underwent washing with deionized water and centrifuging. The solid was put at 100 °C for 12 h then 650 °C for 6 h to remove template agent and Na/SSZ-13 catalyst was obtained. Cu/SSZ-13 was prepared via a two-step wet ion-exchange method. First, Na/SSZ-13 was put in $(NH_4)_2SO_4$ (Purity above 99 wt%, Tianjin Kemiou Chemical Reagent Co., Ltd., China) solution at 80 °C stirred for 4 h and NH_4/SSZ-13 was obtained. NH_4/SSZ-13 was put in $Cu(NO_3)_2$ (purity above 99 wt%, Tianjin Kemiou Chemical Reagent Co., Ltd., China) solution at 80 °C stirred for 1 h and Cu/SSZ-13 was obtained. Every time after the ion-exchange process, the slurry underwent filtering, washing and dried at 100 °C overnight to obtain solid. The obtained Cu/SSZ-13 was calcined at 550 °C for 6 h and this was denoted as fresh Cu/SSZ-13, whose Si/Al ratio is ~13.4 (by XRF) and Cu content is ~1.78 wt% (by ICP).

Table 1. Treatment conditions and BET surface area of different samples

Samples	Treatment conditions	BET surface area (m^2/g)
Cu-F	-	718.2
Cu-S-100-8	250 °C, 100 ppm SO_2, 10% O_2, 3% H_2O in N_2 for 8 h	665.2
R-500-4	500 °C, 10% H_2O in air for 4 h	672.1
R-600-4	600 °C, 10% H_2O in air for 4 h	684.0
R-650-4	650 °C, 10% H_2O in air for 4 h	686.9
R-700-4	700 °C, 10% H_2O in air for 4 h	690.9
R-650-16	650 °C, 10% H_2O in air for 16 h	697.6
R-700-16	700 °C, 10% H_2O in air for 16 h	699.0
R-750-16	750 °C, 10% H_2O in air for 16 h	700.4

In this study, we focused on the stable Cu sulfate decomposition process over Cu/SSZ-13. Therefore, the fresh Cu/SSZ-13 was first sulfated at 250 °C for 8 h in steam containing 10% O_2, 3% H_2O and 100 ppm SO_2. To obtain regenerated samples, the sulfated samples were heated to treatment temperature from room temperature at a ramp rate of 5 °C/min, respectively, and then held for a certain time at the final temperature in wet-air steam containing 10% H_2O. The detailed nomenclatures are shown in Table 1.

2. Catalysts Characterization

Scanning electron microscopy (SEM) images of the samples were recorded by HITACHI S4800 field emission microscope. The samples were fixed on a sample stage with conductive carbon tape and then covered with Au spray.

The powder X-ray diffraction spectra were collected by D8-Focus under Cu-Kα radiation (λ=1.5418A) at a speed of 8°/min. The data were collected in the 2θ range from 5° to 50°.

The specific surface area of catalyst sample was measured by BET method with a sorption analyzer (ASAP 2460) using liquid N_2 at −196 °C.

^{27}Al and ^{29}Si MAS NMR spectra were recorded on a Varian Infinity Plus 300WB spectrometer at 78.13 and 59.57 MHz, respectively, and recorded with a spinning rate of 8 kHz and 4 kHz, respectively. For ^{27}Al and ^{29}Si NMR spectroscopy, $Al(NO_3)_3$ aqueous solution and tetramethylsilane were used as chemical references, respectively. The samples were dehydrated at 250 °C for one day before MAS NMR experiments.

Ex-situ DRIFTs experiments were performed using Nicolet 6700 spectrometer to measure the change of structure. Before each measurement, catalyst sample was pre-treated at 250 °C for 0.5 h with

10% O_2/N_2 from room temperature at a ramp rate of 10 °C/min. The spectra were recorded at 250 °C with the KBr spectrum under the same condition as the background. The DRIFTs spectra were recorded in the range of 4,000-650 cm^{-1} for four scans with a resolution of 4 cm^{-1}. The in-situ DRIFTs experiments were performed via the same instrument to measure the TOT vibrations. Before each measurement, catalyst sample was pre-treated the same treatment as ex-situ DRIFTs. The spectra were recorded at 100 °C after NH_3 adsorption saturation with the catalysts before absorbing NH_3 at the same temperature as background.

The thermal gravimetric analysis experiments were performed using Mettler Toledo thermal gravimetric analyzer to measure the weight change of regenerated and sulfated catalysts. 15 mg sample was placed in a ceramic crucible, then heated from room temperature to 900 °C at a ramp rate of 10 °C/min in a gas flow containing 40 mL/min N_2 and 10 mL/min O_2.

H_2 temperature programmed reduction (H_2-TPR) experiments were conducted for fresh, sulfated and regenerated catalysts. Before the test, samples were pre-treated under a flow of 30 mL/min 5% O_2/N_2 at 250 °C for 30 min after being heated from room temperature to 250 °C with a ramp rate of 10 °C/min and then cooled to room temperature and purified by N_2. The samples were tested under a flow of 10 mL/min 5% H_2/N_2 from 30 °C to 800 °C with a ramp rate of 10 °C/min. The consumption of H_2 was determined by TCD signal intensity.

Electron paramagnetic resonance (EPR) experiments were conducted on Bruker EMXPLUS10/12 to measure the content of isolated Cu^{2+}. The samples were pre-treated in dry air at 250 °C for 24 h, then put in quartz tubes for EPR experiments. The spectra were recorded at −150 °C with a magnetic field swept from 2,000 to 4,000 G, and the frequency was 9.78 GHz. $CuSO_4$ solutions were used as references to calculate the content of isolated Cu^{2+} of catalysts.

3. NH_3-SCR Activity

The NH_3-SCR tests were measured in quartz reactors. 0.1 g catalyst samples (60-80 mesh) and 0.9 g quartz sand (60-80 mesh) were mixed, then put in the reactor. Before each SCR test, the catalyst sample was pre-treated at 250 °C for 30 min in 10% O_2/N_2 and then cooled to 100 °C. The feed gas contained 500 ppm NH_3, 500 ppm NO_x, 3% H_2O, 10% O_2 and N_2 balanced, and the total flow rate was controlled at 1.1 L/min. The inlet and outlet concentrations of NO_x were detected by a Fourier transform infrared spectrometer (MKS-2030). The NO_x conversion was calculated by the following equation:

$$NO_x \text{ conversion } [\%] = \frac{NO_{x,\,inlet} - NO_{x,\,outlet}}{NO_{x,\,inlet}} \times 100\% \quad (1)$$

where $NO_{x,\,inlet}$ is the inlet concentration of NO_x, $NO_{x,\,outlet}$ is the outlet concentration of NO_x.

The NH_3-SCR kinetics experiments were measured in quartz reactors. 0.025 g catalyst samples (80-100 mesh), and 0.125 g quartz sand (80-100 mesh) was mixed and put in the reactor. Before each kinetics experiment, catalyst sample was pre-treated at 250 °C for 30 min in 10% O_2/N_2. The feed gas contained 500 ppm NH_3, 500 ppm NO_x, 3% H_2O, 10% O_2 and N_2 balanced, and the GHSV= 432,000 h^{-1}. The reaction rates of NH_3-SCR could be calculated by the following equation:

$$\text{Rate}[\text{mol } NO_x \cdot g_{catal}^{-1} \cdot s^{-1}] = \frac{X_{NO_x}[\%] \times F_{NO_x}[L_{NO_x} \cdot \text{min}^{-1}]}{m_{catal} \times 60[s \cdot \text{min}^{-1}] \times 22.4[L \cdot \text{mol}^{-1}]} \quad (2)$$

where X_{NO_x} is NO_x conversion [%], F_{NO_x} is NO_x flow rate [$L_{NO_x} \cdot \text{min}^{-1}$], m_{catal} is mass of catalysts.

Turnover frequency (TOF), the moles of NO molecules converted per second by the moles of Cu^{2+} species in Cu/SSZ-13, was calculated by the following equation:

$$TOF[s^{-1}] = \frac{X_{NO_x}[\%] \times F_{NO_x}[L_{NO_x} \cdot \text{min}^{-1}] \times 63.5[g \cdot \text{mol}^{-1}]}{m_{catal}[g] \times M_{Cu(II)}[\%] \times 60[s \cdot \text{min}^{-1}] \times 22.4[L \cdot \text{mol}^{-1}]} \quad (3)$$

where $M_{Cu(II)}$ is the mass fraction of Cu^{2+} in Cu/SSZ-13 (quantified by EPR).

RESULTS

1. CHA Structure Change during Sulfation and Regeneration

1-1. SEM Results

SEM experiments were first conducted for all samples, and the results are shown in Fig. 1. According to the SEM results, the cubic particle size of fresh Cu/SSZ-13 was 0.5-4 μm. And there is no significant difference in morphology among fresh, sulfated and regenerated Cu/SSZ-13 catalysts, although particles slightly aggregated to form secondary particles of >4 μm on R-750-16.

TEM was also performed on the selected samples (Cu-F, Cu-S-100-8, R-750-16). As shown in Fig. S1, no difference could be traced in these samples. All the morphology results above suggest that the sulfation and the regeneration treatment in this study have no significant influence on the texture of the Cu/SSZ-13 catalyst.

1-2. BET and XRD Results

To investigate the structure information of catalysts, BET surface area was measured and XRD experiments were performed. The BET surface area of fresh, sulfated and regenerated catalysts is listed in Table 1. The fresh sample (Cu-F) shows the largest surface area, while the sulfated sample presents the lowest surface area, which is

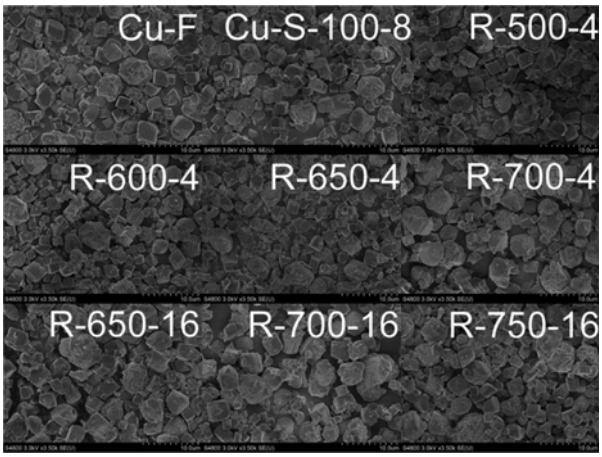

Fig. 1. SEM results for the fresh, sulfated and regenerated Cu/SSZ-13 catalysts.

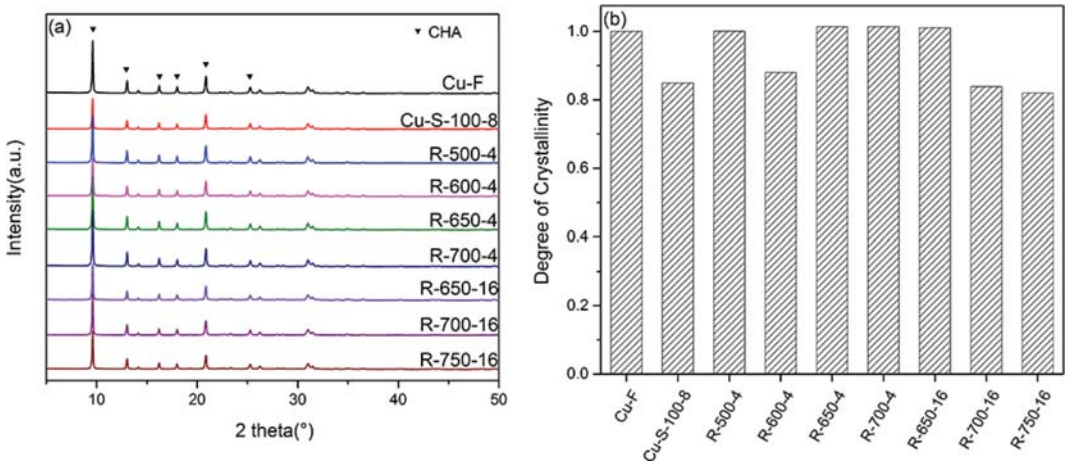

Fig. 2. XRD patterns (a) and crystallinities (b) for the fresh, sulfated and regenerated Cu/SSZ-13 catalysts.

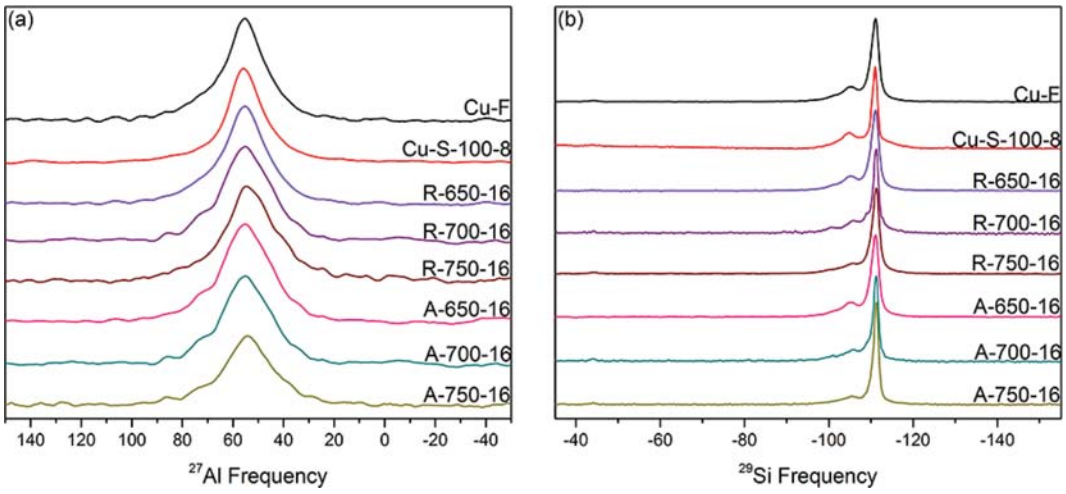

Fig. 3. NMR results of fresh, sulfated, regenerated and aged Cu/SSZ-13 catalysts.

consistent with other reports [16]. This illustrates that the formed sulfur species during sulfation lead to pore plugging but only to a lesser degree. When the sulfated catalyst undergoes regeneration treatment, the surface area of catalyst will increase. Then, the surface area continually increases back to the initial state when sulfated samples are hydrothermally treated at a higher temperature and longer time, which suggests that the content of sulfur species decreases.

To further determine whether sulfation or regeneration will impact the structure of the Cu/SSZ-13 catalysts, XRD experiments were also performed and the results are presented in Fig. 2. Diffraction peaks at 9.6°, 13°, 16.3°, 18°, 20.9° and 25.3° can be observed, which suggests that all samples have a typical chabazite (CHA) structure [19]. According to the former studies, the relative crystallinity of these samples could be estimated using the area of the diffraction peaks [20]. As shown in Fig. 2(b), all samples have similar crystallinity, which reveals that the structures are intact and suggests that sulfation and regeneration have less effect on CHA structure.

1-3. NMR Results

To probe the structural changes upon sulfation and regeneration processes, NMR experiments were conducted to acquire ^{27}Al and ^{29}Si spectra and the results are shown in Fig. 3.

Fig. 3(a) shows ^{27}Al spectra for fresh, sulfated and regenerated ones. In this result, tetrahedrally coordinated framework Al appears at 56 ppm and no feature attributed to octahedrally coordinated extra framework Al at 0 ppm [8,21,22]. Compared with Cu-F, almost no dealumination occurs on sulfation and hydrothermal aging at 650 °C for 16 h, while the extent of dealumination increases progressively with increasing regeneration temperature to 750 °C. Combined with XRD results, it is worth noting that the partial dealumination could not influence the spatial structure integrity.

The corresponding ^{29}Si NMR spectra are displayed in Fig. 3(b). Two features at −104 and −110 ppm appear, which are assigned to $Si(OSi)_3(OAl)$ and $Si(OSi)_4$ [8]. When the hydrothermal aging temperature rises to 700 °C and higher, the −104 ppm feature declines, which is consistent with dealumination shown in Fig. 3(a).

1-4. DRIFTs Results

DRIFTs experiments were performed to probe the -OH and TOT vibrational region using ex-situ and NH_3 adsorption. As shown in ex-situ DRIFTs results (Fig. 4(a)), four bands centered at 3,732, 3,645, 3,604 and 3,576 cm^{-1} can be observed. The bands at 3,732

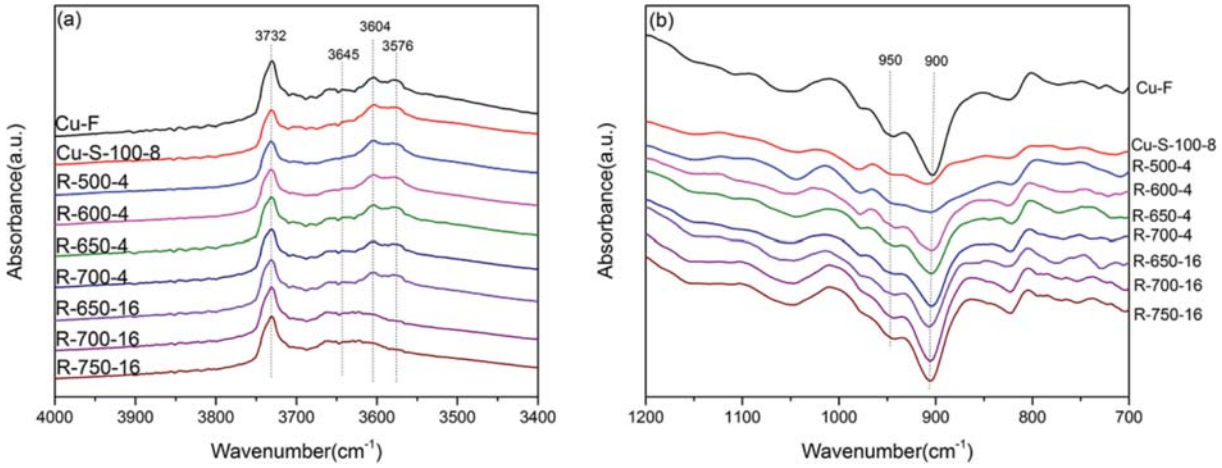

Fig. 4. DRIFTs results of the fresh, sulfated and regenerated Cu/SSZ-13 catalysts: (a) -OH vibrational region and (b) TOT vibrational region perturbed by NH_3 adsorption.

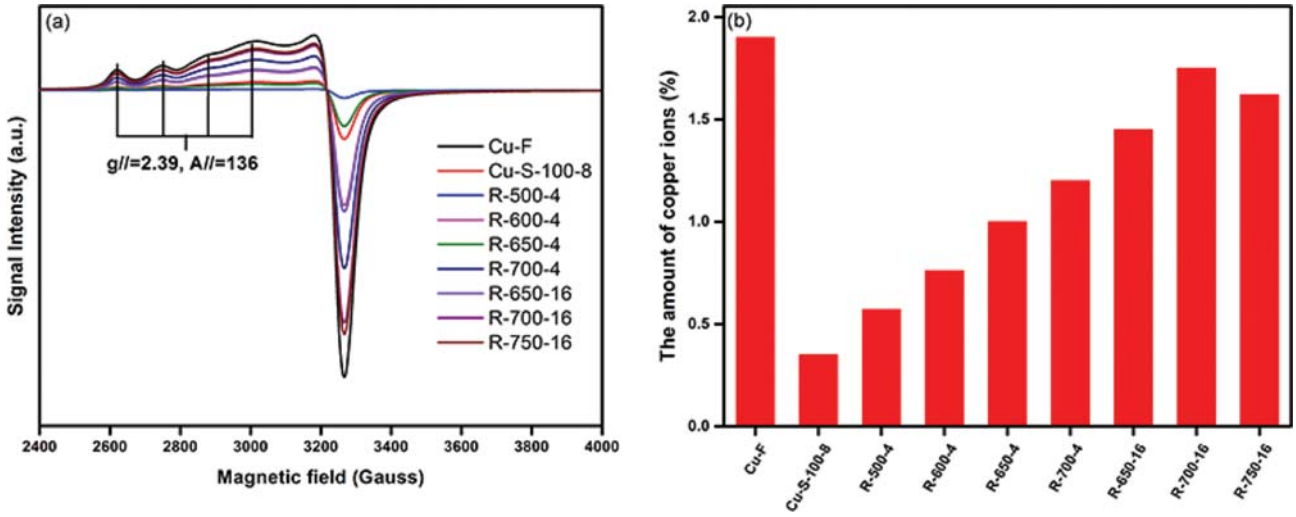

Fig. 5. EPR spectra (a) and quantitating results (b) for fresh, sulfated and regenerated Cu/SSZ-13 catalysts.

cm^{-1} and 3,645 cm^{-1} are attributed to Si-OH and Cu-OH, respectively [23,24]. The bands at 3,604/3,576 cm^{-1} are attributed to Brønsted acid sites (Si-O(H)-Al). As shown in Fig. 4(a), the intensity of Brønsted acid sites does not change after sulfating, while after regenerating at a temperature higher than 700 °C, their intensity obviously decreases because dealumination occurs, which is supported by ^{27}Al NMR results in Fig. 3(a).

The trend of Lewis acid sites can be found in Fig. 4(b); the band at 900 cm^{-1} is associated with Cu^{2+} near six-membered rings (6MRs), and the band at 950 cm^{-1} is associated with Cu^{2+} located in CHA cage, close to 8MRs [14]. The weak intensity of two types of copper ions presence after sulfation illustrates that most of the content of Cu^{2+} in 6MRs or 8MRs lost. Note that the intensity of negative peaks at 950 and 900 cm^{-1} gradually grows after regeneration treatments [25]. The degree of increment increases as the treatment temperature and duration increase. After thermal treatment at 700 and 750 °C for 16 h, the intensity of 900 cm^{-1} recovers to the initial intensity; however, the intensity of 950 cm^{-1} does not. These results reveal that higher temperature and duration help Cu^{2+} in recovering, but not fully recovering.

2. Variation of Copper Species

2-1. EPR Results

It has been demonstrated recently that two types of Cu^{2+} have EPR signal using hydrated catalysts. The same method was used and the results of fresh, sulfated and regenerated Cu/SSZ-13 catalysts are shown in Fig. 5(a). All samples show the same g// and A// value, indicating that the Cu^{2+} shows the same coordination environment [10]. As shown in Fig. 5(b), the sulfated catalyst clearly has the lowest amount of Cu^{2+}. With increasing regeneration temperature and duration, the Cu^{2+} content gradually recovers and reaches the high content on R-700-16. Then, the Cu ions decrease as the regeneration temperature rises at 750 °C for 16 h. This is due to some of Cu^{2+} reforming to CuO at such high temperature aging. The amount of copper ions decreases in the following order: Cu-F (1.9 wt%)> R-700-16 (1.75 wt%)>R-750-16 (1.62 wt%)>R-650-16 (1.45 wt%)> R-700-4 (1.2 wt%)>R-650-4 (1.0 wt%)>R-600-4 (0.76 wt%)>R-500-

4 (0.57 wt%)>Cu-S-100-8 (0.35 wt%). The variation order of copper ion content over catalysts is well correlated with that of sulfate species content, which supports that sulfate species poisoned copper ions.

2-2. H_2-TPR Results

H_2-TPR is a widely used to measure copper species, including different sites of Cu ions, CuO, $CuSO_4$ and other copper species ($CuAlO_2$), over Cu/zeolites. Thus, we used it to probe the overall change trend of different copper species. As shown in Fig. 6(a), Cu-F has three prominent reduction peaks at 220, 340 and 750 °C, which are attributed to the reduction of Z-Cu(OH)$^+$, 2Z-Cu^{2+} and Cu$^+$, respectively [14,26]. Cu ions in 8MRs are about 40% of total Cu ions as shown in Fig. 6(b).

While, new reduction peaks at 260, 400, 500 and 600 °C appear on Cu-S-100-8. Similarly, three reduction peaks at 400, 500 and 600 °C assigned to $CuSO_4$ also showed in H_2-TPR results in our previous study on sulfated Cu/SAPO-34 [16]. These reduction peaks should be attributed to copper sulfate. Since only one type of Cu ion in 6MRs were detected on Cu/SAPO-34, the reduction peak at 260 °C on Cu/SSZ-13 should assign to $CuSO_4$ in 8MRs. The reduction profile of Cu-S-100-8 shows that no Cu ion in 8MRs remains and fewer amounts of Cu ions in 6MRs left on the sulfated sample, suggesting that Cu ions in 8MRs are easily poisoned by sulfur. When sulfated samples went through the regeneration process, the reduction peaks assigned to $CuSO_4$ gradually decreases and no $CuSO_4$ was left on R-700-16 and R-750-16. Meanwhile, another reduction peak at 280 °C attributed to CuO appeared on regenerated samples [16]. The amount of CuO first increases with temperature increasing until R-650-4 and then declines until R-700-16. What's more, the content of CuO rises again when the regeneration temperature is raised to 750 °C.

2-3. TGA Results

To quantify the degree of poisoning and regeneration effect, TGA experiments were performed and the results are presented in Fig. 7. Since Cu/zeolites could absorb water [27], the weight loss that occurs below 200 °C should be assigned to water evaporation. Compared with the TGA curve of Cu-F, the obvious weight loss above 300 °C on sulfated and regenerated samples can be traced. This weight loss should be attributed to decomposition of sulfur species. As shown in DTG results (Fig. 7(b) and (c)), the negative peak at 700 °C is assigned to copper sulfate because the temperature is much closer to the copper sulfate decomposition temperature, which was

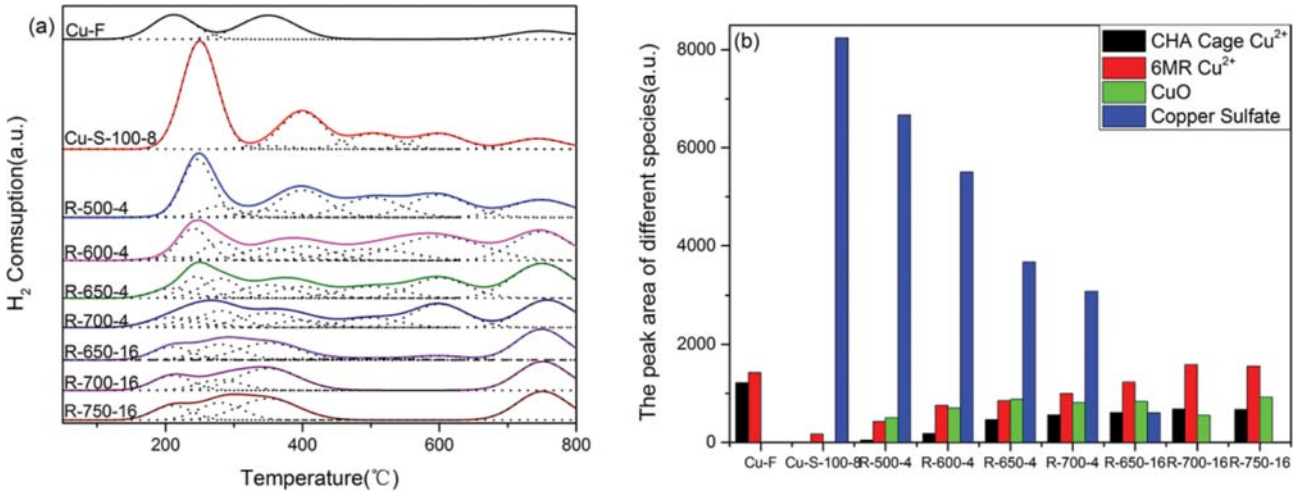

Fig. 6. TPR results for fresh, sulfated and regenerated Cu/SSZ-13 catalysts.

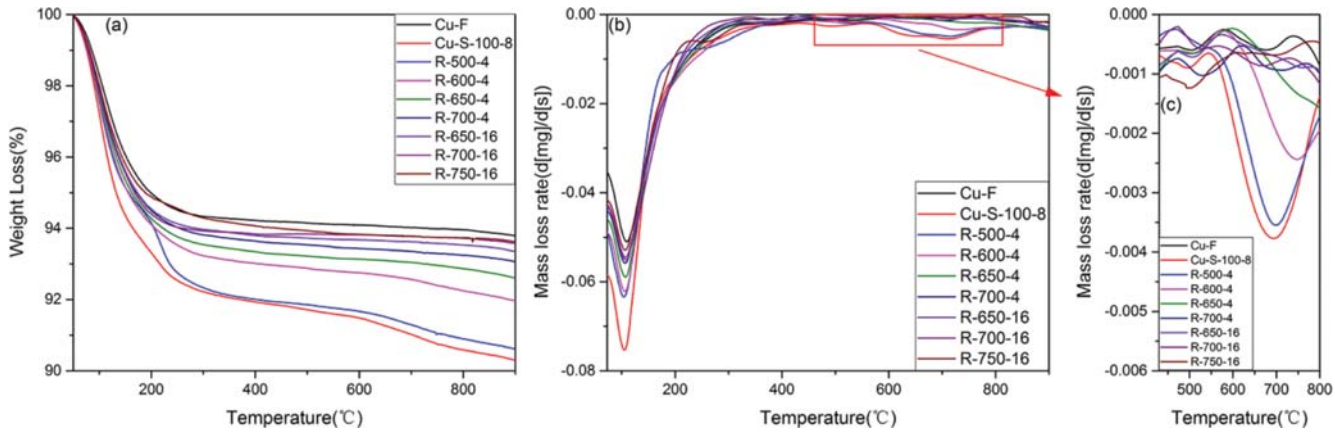

Fig. 7. TGA (a) and DTG (b) results of fresh, sulfated and regenerated Cu/SSZ-13 catalysts.

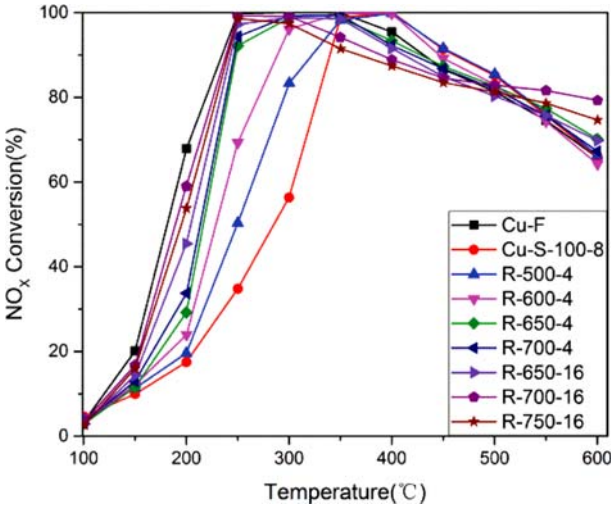

Fig. 8. Standard NH_3-SCR light-off curves for fresh, sulfated and regenerated Cu/SSZ-13 catalysts.

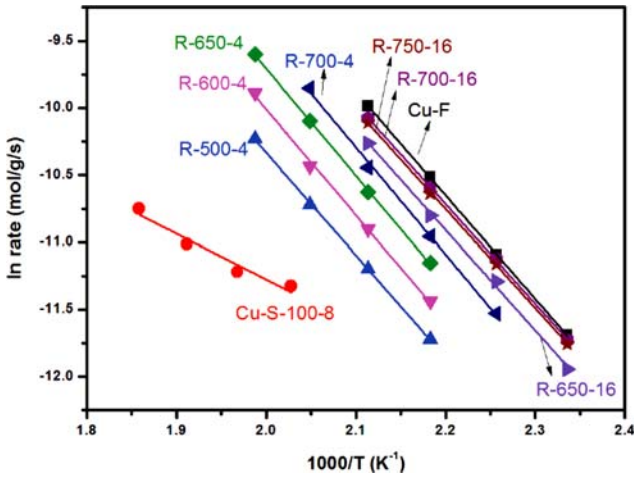

Fig. 9. Arrhenius plots of the SCR reaction rate for fresh, sulfated and regenerated Cu/SSZ-13 catalysts.

carefully studied in our former studies on sulfated Cu/SAPO-34 catalysts [16]. The weight loss above 300 °C of sulfated and regenerated catalysts decreased in this order: Cu-S-100-8 (1.63 wt%)>R-500-4 (1.43 wt%)>R-600-4 (0.98 wt%)>R-650-4 (0.67 wt%)>R-700-4 (0.56 wt%)>R-650-16 (0.43 wt%)>Cu-F (0.35 wt%)≈R-700-16 (0.35 wt%)≈R-750-16 (0.34 wt%). Since the weight losses on Cu-F, R-700-16 and R-750-16 show a similar change, it reveals that no sulfur species remain on R-700-16 and R-750-16. The changes of copper sulfate on samples are consistent with the H_2-TPR results.

3. NH_3-SCR Reaction

3-1. NH_3-SCR Reaction

To comprehensively estimate the regeneration effects, NH_3-SCR activities of fresh, sulfated and regenerated samples were performed and the results are shown in Fig. 8. The fresh Cu/SSZ-13 catalyst shows the highest NO_x conversion. While, Cu-S-100-8 has the lowest activity below 300 °C, which is a common phenomenon on sulfated Cu/CHA catalysts [13]. After sulfated samples were treated at different regeneration conditions, the NH_3-SCR activity gradually increased but never recovered to the initial SCR performance. Note that R-700-16 shows the better NO_x conversion than that of R-750-16 below 300 °C. Besides, the NO_x conversion of R-700-16 and R-750-16 starts to decline above 300 °C.

3-2. Kinetics Experiment

To further probe the NH_3-SCR mechanisms of different samples, the kinetics tests of fresh, sulfated, regenerated catalysts were assessed, and the Arrhenius plots are presented in Fig. 9. The apparent activation energies (Ea, ~64 kJ/mol) are similar for all the catalysts, except for Cu-S-100-8, which suggests that the reaction mechanism does not change. While, the slope of the fitting curve for Cu-S-100-8 obviously changes from ~64 kJ/mol to ~29 kJ/mol, which indicates that the rate-determining step has changed.

DISCUSSION

We performed several characterizations to monitor the CHA structural variation. In a word, the sulfation and regeneration process does not influence the texture and topology structure of catalyst, which is supported by our SEM results in Fig. 1, TEM results in Fig. S1 and XRD results in Fig. 2. However, when regeneration temperature is higher than 700 °C, the dealumination cannot be overlooked, as shown in Fig. 3. As dealumination is the common feature over hydrothermal aged Cu/SSZ-13 [8,24,28-30], it is necessary to distinguish the difference between hydrothermal aging and the regeneration process. Therefore, Cu-F was hydrothermally treated at 700 and 750 °C for 16 h and also tested by ^{27}Al NMR. According to Fig. 3, the results show that the dealumination of the hydrothermally aged sample is more serious than that of the regenerated sample. Even though the reason needs to be further probed, the phenomenon seems useful for the SCR catalysts in the real application.

To comprehend the sulfation and regeneration effect on NO_x conversion, the copper species change and the involved reaction also needs to be well discussed. The active sites, Cu^{2+} and $Cu(OH)^+$, obviously decline after sulfation because of sulfate formation as shown in TGA and H_2-TPR results. After sulfated samples were treated in hydrothermal aging upon regeneration, the formed copper sulfate decomposed. Since copper sulfate decomposes into CuO under thermal treatment [31], copper oxide formed as supported by our H_2-TPR results (Fig. 6). Meanwhile, copper ions, Cu^{2+} and $Cu(OH)^+$, are also formed because CuO could migrate into exchange site during hydrothermal treatment, which is also reported by others [32]. Notably, the ratio of $Cu(OH)^+/Cu^{2+}$ on regenerated catalysts is lower than that on Cu-F, which demonstrates that Cu^{2+} is more favorable to form during migration. One explanation is that Cu^{2+} sites are the priority to occupy as Cu^{2+} is more stable than $Cu(OH)^+$ [25,33]. Another reason is that $Cu(OH)^+$ could convert to Cu^{2+} under hydrothermal aging as reported by Gao et al. [18]. Even though the migration rate will become faster when hydrothermal temperature goes up [9], the increased migration rate is not enough to remove the formed CuO, and, as a result, CuO content continuously increases when the temperature is lower than 650 °C for 4 h. When temperature further increases to 700 °C, CuO content remains unchanged, suggesting that migration rate at 700 °C is

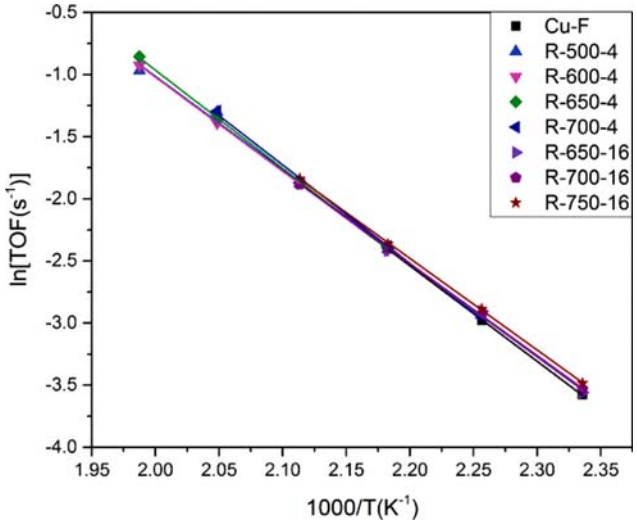

Fig. 10. TOFs results for fresh and regenerated Cu/SSZ-13.

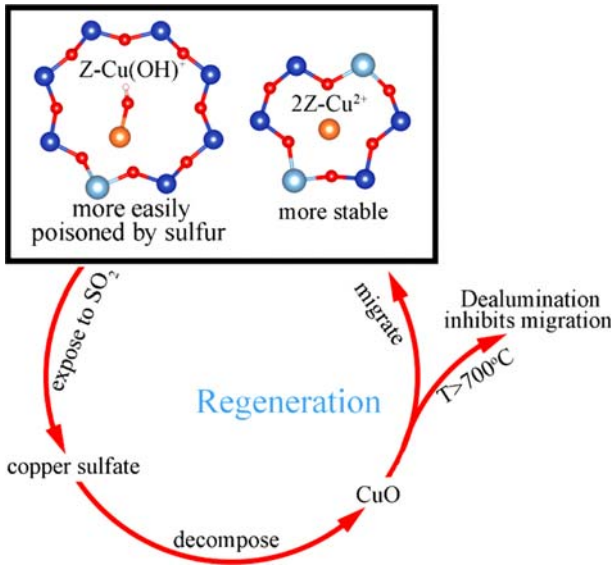

Scheme 1. Mechanism of regeneration for Cu/SSZ-13.

remarkable. Therefore, prolonging the duration to 16 h at 700 °C, CuO content decreases because sulfate completely decomposes and CuO has enough time to transform to exchange sites, although dealumination occurs as shown in ^{27}Al NMR results (Fig. 3(a)). While, the more severe dealumination at 750 °C for 16 h leads to loss of greater amounts of exchange sites and, as a result, copper ion content decreases and CuO amounts increase as shown in our EPR (Fig. 5) and H_2-TPR (Fig. 6) results.

According to the above discussion, the structure-activity relationship on different Cu/SSZ-13 catalysts could be obtained. Except for sulfated sample, all catalysts show the same Ea value, and the only difference among them is the pre-exponential factor. The results suggest that the variation of active sites amounts can affect SCR activity. To justify this hypothesis, the TOFs were calculated based on the EPR and kinetics results (Fig. 5 and Fig. 9). As shown in Fig. 10, the identical TOF values on fresh and regenerated samples strongly support that the increased SCR activity over regenerated catalysts is due to increase of Cu^{2+} ion content. It is noted that Cu-S-100-8 shows the different Ea value compared with fresh catalyst. We recently obtained similar phenomena on high content of sodium-poisoned Cu/SSZ-13 because of the Cu^{2+}/Al less than 0.1 [34]. Thus, in this study, Cu^{2+}/Al value was also calculated on Cu-S-100-8 based on the ICP and EPR results. Since the Cu^{2+}/Al is also less than 0.1 on Cu-S-100-8, the same reason that the rate-determining step on Cu-S-100-8 changes to the formation of Cu-dimer species also receives [13,15]. Above 300 °C, R-700-16 and R-750-16 show a narrow SCR activity window. Combining the fact of the dealumination process and severe loss of Si-O(H)-Al as shown in Fig. 3 and 4, the narrow window is related to the absence of acidity. Based on all the facts, a possible process mechanism of regeneration is proposed, as shown in Scheme 1.

Copper sulfate formed on isolated Cu^{2+} ions and only small amount of 2Z-Cu^{2+} was left during the sulfation process. Correspondingly, copper sulfate content declined after the regeneration process and was completely removed at 700 °C for 16 h. CuO first appears when copper sulfate decomposes and then transforms into exchange sites as copper ions by the migration process. Although the transformation rate is remarkable at 750 °C, CuO amount still increases because of severe dealumination of catalyst. Therefore, considering the Cu/SSZ-13 catalyst should have good low temperature activity and wide temperature window in the practical application, the regeneration temperature needs special attention and should not exceed 700 °C.

CONCLUSIONS

1. The sulfation treatment and lower regeneration temperature will not impact the structure, while when the temperature is higher than 700 °C, obvious dealumination happens.

2. $Cu(OH)^+$ is easily poisoned by sulfur and a small amount of Cu^{2+} remains after sulfation. The reduced copper ions transform into copper sulfate. After the regeneration process, copper sulfate decomposes and the decomposition rate increases with the increasing temperature and duration. When sulfated Cu/SSZ-13 regenerated at 700 °C for 16 h, copper sulfate could fully decompose.

3. Two major reactions, copper sulfate decomposition and migration, occur during regeneration. The migration reaction helps to form copper ions upon regeneration. However, CuO content cannot be fully removed because of severe dealumination appearing at 750 °C.

4. The reduced Cu^{2+} contributes to the SCR activity decline at low temperature, while the loss of acidity is related to the narrow temperature window at high temperature.

ACKNOWLEDGEMENTS

The authors are grateful for the financial support from the National Key Research and Development program (2017YFC 0211302), National Natural Science Foundation of China (No. 21676195), the Science Fund of State Key Laboratory of Engine Reliability (skler-201714).

SUPPORTING INFORMATION

Additional information as noted in the text. This information is available via the Internet at http://www.springer.com/chemistry/journal/11814.

REFERENCES

1. T. Johnson, *SAE Int. J. Engines.*, **6**, 699 (2013).
2. P. Forzatti, I. Nova and E. Tronconi, *Angew. Chem. Int. Ed.*, **48**, 8366 (2009).
3. J. H. Kwak, R. G. Tonkyn, D. H. Kim, J. Szanyi and C. H. F. Peden, *J. Catal.*, **275**, 187 (2010).
4. A. M. Beale, F. Gao, I. Lezcano-Gonzalez, C. H. F. Peden and J. Szanyi, *Chem. Soc. Rev.*, **44**, 7371 (2015).
5. R. Xu, R. Zhang, N. Liu, B. Chen and S. Z. Qiao, *ChemCatChem.*, **7**, 3842 (2016).
6. L. Xie, F. Liu, X. Shi, F.-S. Xiao and H. He, *Appl. Catal. B.*, **179**, 206 (2015).
7. T. Zhang, F. Qiu, H. Chang, X. Li and J. Li, *Catal. Sci. Technol.*, **6**, 6294 (2016).
8. W. Su, Z. Li, Y. Peng and J. Li, *Phys. Chem. Chem. Phys.*, **17**, 29142 (2015).
9. A. M. Beale, I. Lezcano-Gonzalez, W. A. Slawinksi and D. S. Wragg, *Chem. Commun.*, **52**, 6170 (2016).
10. Z. Chen, C. Fan, L. Pang, S. Ming, P. Liu and T. Li, *Appl. Catal. B.*, **237**, 116 (2018).
11. S. Dahlin, C. Lantto, J. Englund, B. Westerberg, F. Regali, M. Skoglundh and Lars J. Pettersson, *Catal. Today*, **320**, 72 (2019).
12. W. Su, Z. Li, Y. Zhang, C. Meng and J. Li, *Catal. Sci. Technol.*, **7**, 1523 (2017).
13. P. S. Hammershøi, Y. Jangjou, W. S. Epling, A. D. Jensen and T. V. W. Janssens, *Appl. Catal. B.*, **226**, 38 (2018).
14. Y. Jangjou, Q. Do, Y. Gu, L.-G. Lim, H. Sun, D. Wang, A. Kumar, J. Li, L. C. Grabow and W. S. Epling, *ACS Catal.*, **8**, 1325 (2018).
15. P. S. Hammershøi, A. D. Jensen and T. V. W. Janssens, *Appl. Catal. B.*, **238**, 104 (2018).
16. C. Wang, J. Wang, J. Wang, T. Yu, M. Shen, W. Wang and W. Li, *Appl. Catal. B.*, **204**, 239 (2017).
17. M. Shen, X. Li, J. Wang, C. Wang and J. Wang, *Ind. Eng. Chem. Res.*, **57**, 3501 (2018).
18. J. Luo, F. Gao, K. Kamasamudram, N. Currier, C. H. F. Peden and A. Yezerets, *J. Catal.*, **348**, 291 (2017).
19. M. M. J. Treacy and J. B. Higgins, in *Collection of simulated xrd powder patterns for zeolites (fifth edition)*, Treacy, M. M. J. and Higgins, J. B. Eds., Elsevier Science B.V., Amsterdam (2007).
20. H. Yu, L. Cheng, J. Yin, S. Yan, K. Liu, F. Zhang, B. Xu and L. Li, *Food Sci. Nutr.*, **1**, 273 (2013).
21. C. Peng, J. Liang, H. Peng, R. Yan, W. Liu, Z. Wang, P. Wu and X. Wang, *Ind. Eng. Chem. Res.*, **57**, 14967 (2018).
22. F. Gao, E. D. Walter, N. M. Washton, J. Szanyi and C. H. F. Peden, *ACS Catal.*, **3**, 2083 (2013).
23. E. Borfecchia, P. Beato, S. Svelle, U. Olsbye, C. Lamberti and S. Bordiga, *Chem. Soc. Rev.*, **47**, 8097 (2018).
24. F. Gao, Y. Wang, N. M. Washton, M. Kollár, J. Szanyi and C. H. F. Peden, *ACS Catal.*, **5**, 6780 (2015).
25. J. Luo, D. Wang, A. Kumar, J. Li, K. Kamasamudram, N. Currier and A. Yezerets, *Catal. Today*, **267**, 3 (2016).
26. J. H. Kwak, H. Zhu, J. H. Lee, C. H. F. Peden and J. Szanyi, *Chem. Commun.*, **48**, 4758 (2012).
27. M. Shen, Y. Zhang, J. Wang, C. Wang and J. Wang, *J. Catal.*, **358**, 277 (2018).
28. J. H. Kwak, D. Tran, S. D. Burton, J. Szanyi, J. H. Lee and C. H. F. Peden, *J. Catal.*, **287**, 203 (2012).
29. S. J. Schmieg, S. H. Oh, C. H. Kim, D. B. Brown, J. H. Lee, C. H. F. Peden and D. H. Kim, *Catal. Today*, **184**, 252 (2012).
30. Y. J. Kim, J. K. Lee, K. M. Min, S. B. Hong, I.-S. Nam and B. K. Cho, *J. Catal.*, **311**, 447 (2014).
31. K. Wijayanti, K. Xie, A. Kumar, K. Kamasamudram and L. Olsson, *Appl. Catal. B.*, **219**, 142 (2017).
32. D. Wang, F. Gao, C. H. F. Peden, J. Li, K. Kamasamudram and W. S. Epling, *ChemCatChem.*, **6**, 1579 (2014).
33. L. Ma, Y. Cheng, G. Cavataio, R. W. McCabe, L. Fu and J. Li, *Chem. Eng. J.*, **225**, 323 (2013).
34. C. Wang, J. Wang, J. Wang, Z. Wang, Z. Chen, X. Li, M. Shen, W. Yan and X. Kang, *Catal.*, **8**, 593 (2018).

Supporting Information

Effects of regeneration conditions on sulfated CuSSZ-13 catalyst for NH_3-SCR

Meiqing Shen[*,,***], Zhixin Wang[*], Xinhua Li[*], Jiaming Wang[*], Jianqiang Wang[*], Chen Wang[****,†], and Jun Wang[*,†]**

*Key Laboratory for Green Chemical Technology of State Education Ministry, School of Chemical Engineering & Technology, Tianjin University, Tianjin 300350, P. R. China
**Collaborative Innovation Centre of Chemical Science and Engineering (Tianjin), Tianjin 300350, P. R. China
***State Key Laboratory of Engines, Tianjin University, Tianjin 300350, P. R. China
****School of Environmental and Safety Engineering, North University of China, Taiyuan 030051, P. R. China
(*Received 13 February 2019 • accepted 21 May 2019*)

Transmission electron microscope (TEM) images of samples were recorded by JEM-2100F field emission electron microscope operated at 200 kV. The sample powder was dispersed on carbon film on Cu TEM grid. The results are shown in Fig. S1.

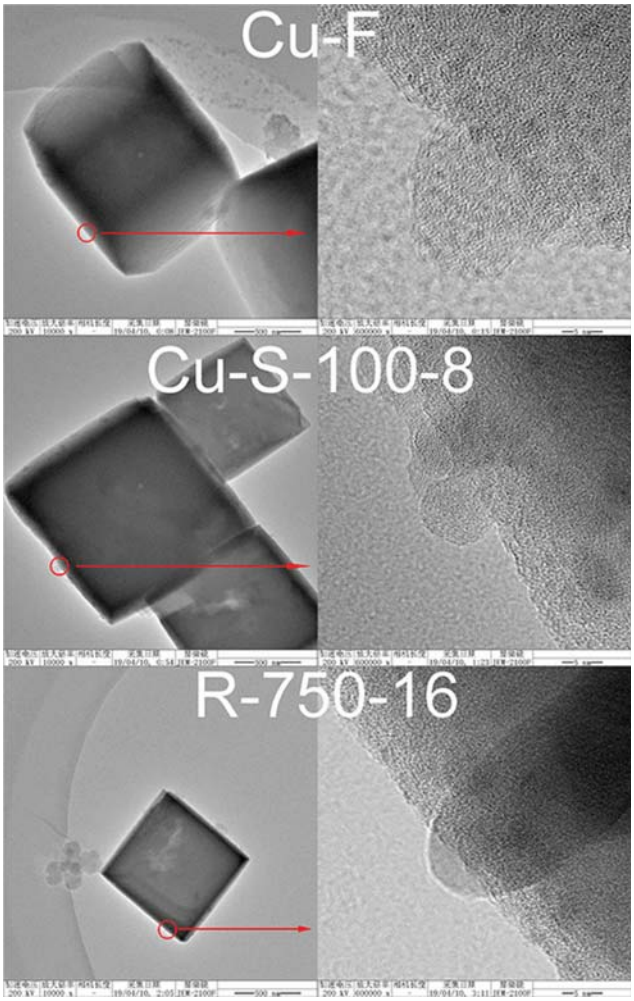

Fig. S1. TEM results for the Cu-F, Cu-S-100-8 and R-750-16 samples.